Struct Multidisc Optim 19, 50–63

Optimal design of beam reinforced composite structures under elasto-plastic loading conditions

C.A. Conceição António, J. Trigo Barbosa, and L. Simas Dinis

Abstract A design optimization process for elasto-plastic material behaviour of laminate composite structures, made of thermoplastic resins, is described. The approach considers two optimization levels. At the first level the geometric linear behaviour under elasto-plastic loading conditions is adopted in order to obtain the optimal solution as a function of ply angles of the plates or shallow shells. At this stage the objective is to recover the plastic zones using only the anisotropic material properties. At the second level the ply thickness of the plates or shallow shells and the height and width of the reinforcement beams are changed to structure weight minimization, under the constraints of maximum allowed displacement or maximum strain-stress level related with amount of plastic zone, without structural plastic collapse or geometric instability in plastic loading conditions. It is expected that contradictory objectives, as minimum elasto-plastic energy and structural weight, are satisfied.

1 Introduction

The increasing interest in thermoplastic composites operating in extremely severe mechanical and thermal environments, has brought more attention to the design of structures made of these materials. It is a well-known fact that thermoplastic composites have ameliorated mechanical properties at high temperatures owing to the increased ductility of the matrix system (Tenney *et al.* 1989; Yoon and Sun 1991). Therefore, the characterization of the elasto-plastic response is indispensable in the limit analysis stage, which must be performed along the reliable design processes for composite structures involving plasticity effects in the nonlinear behaviour (Min 1981; Dvorak and Bahei-El Din 1982). The study of the optimal design of thermoplastic composite structures is an emerging research field and few authors (Oblak *et al.* 1993; Ohsaki and Arora 1994; Selyugin 1995) have presented results in this area. The present paper is devoted to optimization of beam reinforced plates and shallow shells structures made of nonwork-hardening elasto-plastic materials. Deformation plasticity theory is used for developing optimization algorithms.

Received August 24, 1998
Revised manuscript received January 18, 1999

C.A. Conceição António, J. Trigo Barbosa, and L. Simas Dinis

Faculdade de Engenharia da Universidade do Porto, Rua dos Bragas, P–4099 Porto Codex, Portugal

2 Structural analysis

In this work, composite materials are considered for the construction of beam reinforced plates and shallow shell structures, under infinitesimal strains and material nonlinear behaviour.

The finite element method is used for the spatial discretization of the reinforced plate coupled with the Mindlin plate and Timoshenko beam theories, which takes into account shear deformation effects (Zienkiewicz and Taylor 1994); in the present analysis a nine-noded plate element and a three-noded beam element are adopted in the discretization process. It is assumed that the stiffeners are monolithically connected to the plate along the borders of plate elements. Those assumptions imply that identical displacement fields are produced at the junction between the plate and the stiffeners.

The model is extended, using the Marguerre shallow shell theory (Marguerre 1938), to enable the behaviour of shallow shells to be examined using a Mindlin formulation.

The structure is subdivided in layers throughout the thickness, allowing the eventual variation of the material properties in the beams and plate as well as a more precise modelling of the nonlinear response. An elasto-plastic model is adopted in order to represent the material nonlinear behaviour and the Hill yield function is employed for anisotropic materials (Hill 1950).

The mathematical treatment of the nonlinear equilibrium equations, based on a total Lagrangean approach of the virtual work principle, is done resorting to a displacement based finite element formulation (Bathe 1996). The

solution of the resulting nonlinear equation system is accomplished by use of the Newton-Raphson method and related modified versions (Zienkiewicz and Taylor 1994).

2.1 Reinforced laminate

The behaviour of the reinforced laminate is accessed through the combined action of two structural components: the plate and the reinforcement beam. All degrees of freedom, as well as the flexural properties of the system are defined at the reference plane which is chosen to coincide with the plate midsurface, thus implying that the stiffeners are relatively shallow.

2.1.1 Plate element

The displacements $\mathbf{u} = [u, v, w]^T$ in a typical point (x, y, z) of the plate are expressed as functions of the midplane translations $\hat{u}$, $\hat{v}$ and $\hat{w}_1$, and independent normal rotations Θ_x and Θ_y, in xz and yz planes, respectively, Fig. 1a, as

$$\mathbf{u} = \begin{bmatrix} u \\ v \\ w \end{bmatrix} = \begin{bmatrix} \hat{u}(x,y) - z\Theta_x(x,y) \\ \hat{v}(x,y) - z\Theta_y(x,y) \\ \hat{w}_1(x,y) + \hat{w}_0(x,y) \end{bmatrix} , \tag{1}$$

where $\hat{w}_0$ defines the midplane initial deflection of the plate before deformation takes place.

Introducing the von Kármán assumptions (Fung 1965) in Green's strain tensor (Crisfield 1991), the strain vector $\boldsymbol{\varepsilon}$ for a Mindlin shallow shell can be expressed as

$$\boldsymbol{\varepsilon} = [\varepsilon_x, \varepsilon_y, \gamma_{xy}, \gamma_{xz}, \gamma_{yz}]^T = \begin{bmatrix} \varepsilon_p \\ \varepsilon_s \end{bmatrix} = \begin{bmatrix} \varepsilon_m + z\varepsilon_b + \varepsilon_I \\ \varepsilon_s \end{bmatrix} , \tag{2}$$

ε_m and ε_b being, respectively, the membrane and bending components of linear midplane strains, ε_s the shear transverse strains and, finally, ε_I the linear contributions of the initial deformation to the midplane strains, were defined by Pica *et al.* (1980) and Pica and Wood (1980).

Under elastic conditions the Piola-Kirchhoff stress vector, $\boldsymbol{\sigma}$, associated with Green's strains $\boldsymbol{\varepsilon}$ of (2), is calculated assuming that the material is orthotropic with the material axes 1,2 being parallel to the midsurface of the plate, considered as the xy plane, and the material axis 3 being coincident with z; the stress-strain relation (Huang 1989) has the form

$$\boldsymbol{\sigma} = [\sigma_x, \sigma_y, \tau_{xy}, \tau_{xz}, \tau_{yz}]^T = \mathbf{D}\boldsymbol{\varepsilon} = \mathbf{T}'^T \overline{\mathbf{D}} \mathbf{T}' \boldsymbol{\varepsilon} , \tag{3}$$

where $\mathbf{D}$, the general elasticity matrix, depends on the matrix of elastic constants $\overline{\mathbf{D}}$, which relates stresses and strains referred to the material axes 1,2,3, having the nonzero terms defined by the following expressions:

$$\overline{D}_{11} = E_1/\Delta , \quad \overline{D}_{22} = E_2/\Delta , \quad \overline{D}_{12} = \nu_{12}\overline{D}_{22} ,$$

$$\overline{D}_{33} = G_{12} , \quad \overline{D}_{44} = k_{13}G_{13} , \quad \overline{D}_{55} = k_{23}G_{23} ,$$

$$\Delta = 1 - \nu_{12}\nu_{21} , \tag{4}$$

in which E_1 and E_2 are, respectively, Young's moduli in the 1 and 2 directions, ν_{ij} is Poisson's ratio for transverse strain in the i-direction when stressed in the j-direction and G_{13} and G_{23} are the shear moduli in the 13 and 23 planes, respectively; the terms k_{13} and k_{23} are shear correction factors in the 13 and 23 planes, respectively. The stress transformation matrix $\mathbf{T}'$, which relates the principal material system (1,2,3) with the global system (x, y, z), is a function of the angle Θ formed by positive direction of axis 1 with the positive direction of axis x and is defined by Huang (1989).

2.1.2 Beam element

The beam element, Fig. 1b, is assumed to be symmetric about local $x'z$ plane, weak in bending related with displacements parallel to the plane of the plate, so that the corresponding flexural rigidity is neglected, and that local buckling of the stiffeners and cross-section distortions can be ignored. A local system of axes $x'y'z$, where $x'y'$ plane is parallel to the global xy plane, is considered to model structural behaviour of the stiffener.

The admitted displacements in a typical point (x', y', z) of the stiffener are

$$\overline{u} = \overline{\hat{u}}(x') - z\Theta_{x'}(x') , \quad w = \hat{w}_1(x') + \hat{w}_0(x') , \tag{5}$$

where $\overline{\hat{u}}$ is the axial displacement of the centroid, $\Theta_{x'}$ is the rotation about y' local axis and the deflections $\hat{w}_1$ and $\hat{w}_0$ have an analogous meaning as that defined above. Assuming that the local axes x', y' of the beam do not coincide with the reference axes x, y but are rotated by an angle α, the displacements of the beam centroid, $\overline{\mathbf{d}}_i = [\overline{\hat{u}}, \hat{w}_1, \Theta_{x'}, \Theta_{y'}]_i^T$, are expressed in terms of the global displacements of the plate i-th node, $\mathbf{d}_i = [\hat{u}, \hat{v}, \hat{w}_1, \Theta_x, \Theta_y]_i^T$, as

$$\overline{\hat{u}}_i = \hat{u}_i \cos\alpha + \hat{v}_i \sin\alpha ,$$

$$\begin{bmatrix} \Theta_{x'} \\ \Theta_{y'} \end{bmatrix}_i = \begin{bmatrix} \cos\alpha & \sin\alpha \\ -\sin\alpha & \cos\alpha \end{bmatrix} \begin{bmatrix} \Theta_x \\ \Theta_y \end{bmatrix}_i . \tag{6}$$

Similarly as in (2), the strain vector used for the present Timoshenko shallow beam is

$$\boldsymbol{\varepsilon}' = \begin{bmatrix} \boldsymbol{\varepsilon} \\ \varepsilon_t \end{bmatrix} = \begin{bmatrix} \varepsilon_{x'} \\ \gamma_{x'z} \\ \varepsilon_t \end{bmatrix} = \begin{bmatrix} \varepsilon_m + z\varepsilon_b + \varepsilon_I \\ \gamma_{x'z} \\ \varepsilon_t \end{bmatrix} =$$

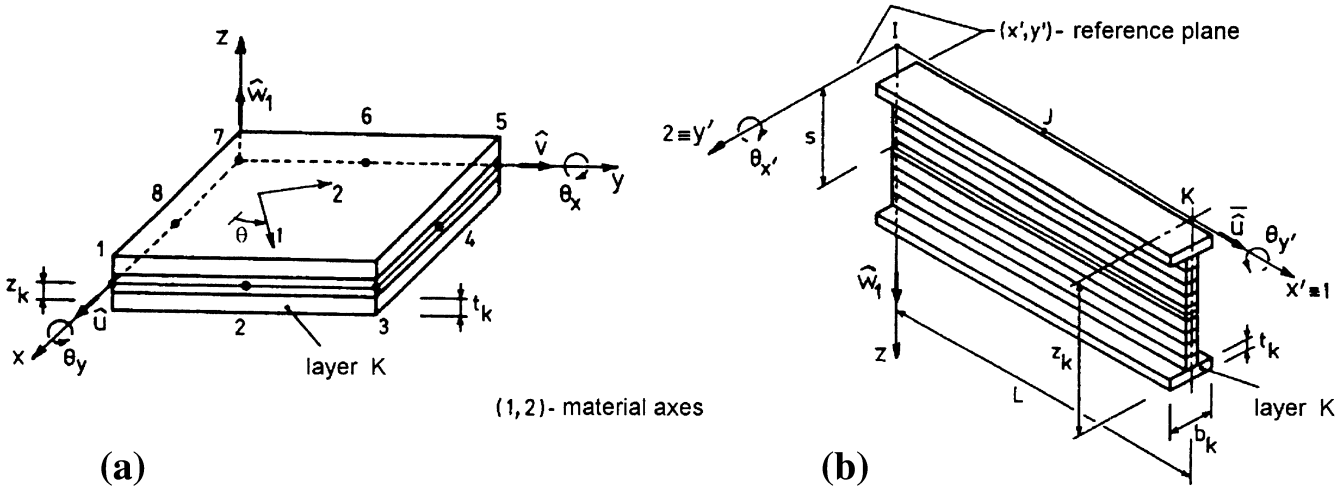

Fig. 1 Reinforced laminate: (a) plate element and (b) beam element

$$\begin{bmatrix} \partial\overline{\hat{u}}/\partial x' - z\partial\Theta_{x'}/\partial x' + \partial\hat{w}_1/\partial x'\partial\hat{w}_0/\partial x' \\ \partial\hat{w}_1/\partial x' - \Theta_{x'} \\ \partial\Theta_{y'}/\partial x' \end{bmatrix} , \tag{7}$$

in which ε_t is the torsional strain due to the variation of the axial rotation $\Theta_{y'}$ along x' axis.

In order to derive the stress-strain relations for the stiffener it is considered, in this case, that the material axes are coincident with the beam local axes, $1 \equiv x'$, $2 \equiv y'$ and $3 \equiv z$. So, assuming that only $\sigma_{x'}$ and $\tau_{x'z}$ are the nonzero terms of the stress vector $\boldsymbol{\sigma}$, the expressions (3) and (4) become

$$\boldsymbol{\sigma} = \begin{bmatrix} \sigma_{x'} \\ \tau_{x'z} \end{bmatrix} = \mathbf{D} \begin{bmatrix} \varepsilon_{x'} \\ \gamma_{x'z} \end{bmatrix} = \mathbf{D}\boldsymbol{\varepsilon} , \tag{8}$$

or

$$\sigma_{x'} = \frac{\overline{D}_{11} - (\overline{D}_{12})^2}{\overline{D}_{22}} \varepsilon_{x'} , \quad \tau_{x'z} = \overline{D}_{44}\gamma_{x'z} , \tag{9}$$

while the term ε_t induces a torsional moment $M_{y'}$ which must be treated in an elastic manner. For homogeneous material the torsion is described by the well-known expression

$$M_{y'} = GJ\varepsilon_t , \tag{10}$$

where GJ is the torsional rigidity of the stiffener.

2.2 Layered model

The structure is subdivided in layers throughout the thickness, Fig. 1, each layer contains stress points on its midsection. The stress components and stiffness contributions are computed at these stress points and are assumed to be constant over the thicknesses of each layer, so that the actual stress distribution over the structure thickness is modelled by a piecewise constant approximation (Huang 1989) in the integral over the thickness is used a mid-ordinate rule.

2.3 Elasto-plastic model

The elasto-plastic material behaviour is described resorting to the mathematical theory of plasticity (Hill 1950), and adopts an incremental relation between stresses and strains, a yield criterion, the nonexistence of material hardening and an associated flow rule to describe the plastic flow after yielding.

The yield criterion employed for anisotropic materials is a generalised form of the Huber-Mises law (Owen and Figueiras 1983) and can be written in the general form

$$F(\boldsymbol{\sigma}) = f(\boldsymbol{\sigma}) - Y = 0 , \tag{11}$$

where Y is the yield level and $f(\boldsymbol{\sigma})$ is a yield function that can be defined in terms of the stresses referred to the material axes 1,2,3 as

$$f^2(\boldsymbol{\sigma}) = \overline{\sigma}^2 = a_1\sigma_1^2 + 2a_{12}\sigma_1\sigma_2 + a_2\sigma_2^2 +$$

$$a_3\tau_{12}^2 + a_4\tau_{13}^2 + a_5\tau_{23}^2 = \boldsymbol{\sigma}_{1,2,3}^T \mathbf{A}\boldsymbol{\sigma}_{1,2,3} , \tag{12}$$

in which $\mathbf{A}$ is the matrix of the anisotropic parameters, determined by six independent yield tests, and $\overline{\sigma}$ is the effective stress, usually taken as the uniaxial yield stress in 1-direction.

If the material axes 1,2 are rotated of an angle Θ in relation to the reference axes x, y, then the transformation of both stresses and matrix $\mathbf{A}$ to the global axes is necessary. So, the obtained yield criterion can be rewritten as

$$f^2(\boldsymbol{\sigma}) = \overline{\sigma}^2 = \boldsymbol{\sigma}^T\mathbf{T}^T\mathbf{A}\mathbf{T}\boldsymbol{\sigma} = \boldsymbol{\sigma}^T\overline{\mathbf{A}}\boldsymbol{\sigma} , \tag{13}$$

where $\mathbf{T}$ is the strain transformation matrix (Huang 1989) which relates the material system (1,2,3) with the global system (x, y, z).

The total strain increment $\mathrm{d}\,\varepsilon$ is, in this case, the sum of the elastic, $\mathrm{d}\,\varepsilon^e$, and plastic, $\mathrm{d}\,\varepsilon^p$, components, so that

$$\mathrm{d}\,\varepsilon = \mathrm{d}\,\varepsilon^e + \mathrm{d}\,\varepsilon^p\,, \tag{14}$$

being the plastic strain increment given by the associated flow rule

$$\mathrm{d}\,\varepsilon^p = \mathrm{d}\,\lambda \frac{\partial f}{\partial \boldsymbol{\sigma}} = \mathrm{d}\,\lambda \mathbf{a}\,, \tag{15}$$

where $\mathrm{d}\,\lambda$ and $\mathbf{a}$ are, respectively, the plastic multiplier and the flow vector.

The elasto-plastic incremental stress-strain relation is obtained knowing that

$$\mathrm{d}\,F = \mathbf{a}^T \mathrm{d}\,\boldsymbol{\sigma} = 0\,, \tag{16}$$

and

$$\mathrm{d}\,\boldsymbol{\sigma} = \mathbf{D}\mathrm{d}\,\varepsilon^e = \mathbf{D}\mathrm{d}\,\varepsilon - \mathrm{d}\,\lambda \mathbf{D}\mathbf{a}\,, \tag{17}$$

and, finally, the manipulation of (16) and (17) leads to

$$\mathrm{d}\,\boldsymbol{\sigma} = \mathbf{D}^{ep}\mathrm{d}\,\varepsilon = \left[\mathbf{D} - \frac{\mathbf{D}\mathbf{a}\mathbf{a}^T\mathbf{D}}{\mathbf{a}^T\mathbf{D}\mathbf{a}}\right] \mathrm{d}\,\varepsilon\,. \tag{18}$$

As concerns to the stiffener only the longitudinal and transverse shear stresses are assumed to induce material plasticity.

3
Nonlinear equilibrium equations

The discretized nonlinear equilibrium equations to be solved are derived using a total Lagrangean formulation of the finite element method, where the nodal displacements $\mathbf{d}$ are referred to the initial structure configuration and loading is assumed to be conservative, as (Zienkiewicz and Taylor 1994)

$$\Psi(\mathbf{d}) = \int_V \mathbf{B}^T \boldsymbol{\sigma}\mathrm{d}\,V + \int_L \mathbf{B}_t^T M_{y'}\mathrm{d}\,L - \mathbf{F} =$$

$$\mathbf{r}(\mathbf{d}) - \mathbf{F} \neq \mathbf{0}\,, \tag{19}$$

where $\Psi(\mathbf{d})$ is the residual force vector, $\mathbf{r}(\mathbf{d})$ are the equivalent nodal forces referred to the actual stress distribution, $\mathbf{F}$ is the equivalent nodal force vector due to exterior loads and $\mathbf{B}$ is the strain matrix; the line integral in (19) denotes the effect of torsional strain in beam section on the total deformation energy of the structure. A detailed description of the construction of matrix $\mathbf{B}$ for the plate element was presented by Pica *et al.* (1980) and Pica and Wood (1980).

Adopting a similar procedure, the strain matrix for the beam element, which relates the strain variation to the virtual global nodal displacements $\delta\mathbf{d}$, can be derived substituting (6) in a discretized form of $\delta\varepsilon'$ as

$$\delta\varepsilon = \begin{bmatrix}\delta\varepsilon_{x'} \\ \delta\gamma_{x'z}\end{bmatrix} = \mathbf{B}_0\delta\mathbf{d} = \sum_{i=1}^{3}\mathbf{B}_{0i}\delta\mathbf{d}_i =$$

$$\sum_{i=1}^{3}\begin{bmatrix}\mathbf{B}_m + z\mathbf{B}_f + \mathbf{B}_I \\ \mathbf{B}_s\end{bmatrix}_i \delta\mathbf{d}_i\,, \tag{20}$$

$$\delta\varepsilon_t = \mathbf{B}_t\delta\mathbf{d} = \sum_{i=1}^{3}\mathbf{B}_{ti}\delta\mathbf{d}_i\,, \tag{21}$$

where the corresponding submatrices associated with node i may be written as

$$\mathbf{B}_{mi} = \frac{\partial N_i}{\partial x'}\begin{bmatrix}\cos\alpha & \sin\alpha & 0 & 0 & 0\end{bmatrix}\,, \tag{22}$$

$$\mathbf{B}_{fi} = \frac{\partial N_i}{\partial x'}\begin{bmatrix}0 & 0 & 0 & -\cos\alpha & -\sin\alpha\end{bmatrix}\,, \tag{23}$$

$$\mathbf{B}_{si} = \begin{bmatrix}0 & 0 & \dfrac{\partial N_i}{\partial x'} & -N_i\cos\alpha & -N_i\sin\alpha\end{bmatrix}\,, \tag{24}$$

$$\mathbf{B}_{Ii} = \frac{\partial \hat{w}_{0i}}{\partial x'}\begin{bmatrix}0 & 0 & \dfrac{\partial N_i}{\partial x'} & 0 & 0\end{bmatrix}\,, \tag{25}$$

$$\mathbf{B}_{ti} = \frac{\partial N_i}{\partial x'}\begin{bmatrix}0 & 0 & 0 & -\sin\alpha & \cos\alpha\end{bmatrix}\,. \tag{26}$$

In the present infinitesimal deformation problem the strain matrix is a constant matrix and $\boldsymbol{\sigma}$ is a function of $\mathbf{d}$.

4
Nonlinear solution algorithm

The solution of (19) is sought using the Newton-Raphson method (Zienkiewicz and Taylor 1994), which is an incremental and iterative technique where the exterior loads are incrementally applied. For each load level the equations are approximated by a series of linear solutions and an iterative process is performed in order to reduce the errors to be transfered to the next load level.

Denoting by $\mathbf{d}_i$ an estimate of nodal displacements for the i-th iteration of a load step, the corresponding residual forces are $\Psi(\mathbf{d}_i) \neq \mathbf{0}$ and an improved solution $\mathbf{d}_{i+1}$ for the displacements is obtained as

$$\mathbf{d}_{i+1} = \mathbf{d}_i + \delta\mathbf{d}_i = \mathbf{d}_0 + \Delta\mathbf{d}_i\,, \tag{27}$$

where $\mathbf{d}_0$ is the displacement solution at the end of previous increment,

$$\delta\mathbf{d}_i = -\left.\frac{\partial\Psi(\mathbf{d})}{\partial\mathbf{d}}\right|_i \Psi(\mathbf{d}_i) = -\mathbf{K}_{Ti}^{-1}\Psi(\mathbf{d}_i) \tag{28}$$

is the iterative variation of the displacements, $\mathbf{K}_{Ti}$ is the assembled tangent stiffness matrix of the structure and

$\Delta\mathbf{d}_i$ are the incremental displacements. The updated displacements are used to evaluate the current stresses $\boldsymbol{\sigma}_{i+1}$ and hence the new residual forces Ψ_{i+1} from (19). The iteration process will be stopped and the converged solution will be reached for the current load level, when suitable predefined convergence criteria will be attained and the residual forces are sufficiently close to zero; in the present analysis residual forces are compared with external applied forces at each iteration.

The Newton-Raphson method demands repeated calculation and inversion of $\mathbf{K}_T$. Therefore, some modified forms can be considered, as the KT1, where the tangent stiffness matrix is actualised only on the first iteration of each load increment, and the KT2 whereby $\mathbf{K}_T$ is calculated once only on the second iteration.

5
Tangent stiffness matrix

The definition of the tangential stiffness matrix $\mathbf{K}_T$ for the plate element is quite well described by Pica *et al.* (1980) and Pica and Wood (1980).

As concerns the beam element the variation of Ψ with respect to a displacement variation $\delta\mathbf{d}$ leads to

$$\mathbf{K}_T = \mathbf{K}_0 + \mathbf{K}_t \,, \tag{29}$$

being

$$\mathbf{K}_0 = \int_V \mathbf{B}_0^T \mathbf{D}^{ep} \mathbf{B}_0 \mathrm{d}\, V = \int_V \begin{bmatrix} \mathbf{B}_m + z\mathbf{B}_f + \mathbf{B}_I \\ \mathbf{B}_s \end{bmatrix}^T \mathbf{D}^{ep} \begin{bmatrix} \mathbf{B}_m + z\mathbf{B}_f + \mathbf{B}_I \\ \mathbf{B}_s \end{bmatrix} \mathrm{d}\, V \,, \tag{30}$$

the infinitesimal (deformation) elasto-plastic stiffness matrix and

$$\mathbf{K}_t = \int_L \mathbf{B}_t^T \overline{GJ} \mathbf{B}_t \mathrm{d}\, L \,, \tag{31}$$

the elastic torsional stiffness matrix, where $\overline{GJ}$ represents the equivalent torsional rigidity of the beam.

6
Stress computation in elasto-plasticity

At the end of the i-th iteration of the current load step and assuming that the material has an elastic behaviour, a trial stress state is obtained from the value $\boldsymbol{\sigma}_0$ at the final of the previous load level, that is

$$\boldsymbol{\sigma}^E = \boldsymbol{\sigma}_0 + \Delta\boldsymbol{\sigma}^E = \boldsymbol{\sigma}_0 + \mathbf{D}\mathbf{B}\Delta\mathbf{d} \,, \tag{32}$$

where $\Delta\boldsymbol{\sigma}^E$ is the elastic estimate for the incremental stresses.

If $f(\boldsymbol{\sigma}^E) < Y$ the stress point is elastic and the estimate (32) is correct. Otherwise the yield surface has been trespassed during the trial stress incrementation and the contact stress state $\boldsymbol{\sigma}^C$, with $f(\boldsymbol{\sigma}^C) = Y$, must be computed as

$$\boldsymbol{\sigma}^C = \boldsymbol{\sigma}^E - \Delta\boldsymbol{\sigma}^{exc} = \boldsymbol{\sigma}^E - R\Delta\boldsymbol{\sigma}^E \,, \tag{33}$$

where R is the reduction factor

$$R = \left\{ \left[\frac{\partial f(\boldsymbol{\sigma})}{\partial \boldsymbol{\sigma}} \right]^T \Delta\boldsymbol{\sigma} \right\}^{-1} [f(\boldsymbol{\sigma}) - Y] \,, \tag{34}$$

referred to the trial stress state $\boldsymbol{\sigma} = \boldsymbol{\sigma}^E$. An improved estimate for R is suggested by Marques (1984), to be considered when the yield function is nonlinear on $\boldsymbol{\sigma}$.

The stress point is then brought back to the yield surface by the reduction of the excess stress $\Delta\boldsymbol{\sigma}^{exc}$, which is achieved adopting a subincrementation procedure whereby $\Delta\boldsymbol{\sigma}^{exc}$ is subdivided in m parts. So, the reduced incremental stresses $\Delta\boldsymbol{\sigma}^r$ are given by

$$\Delta\boldsymbol{\sigma}^r = \sum_{k=1}^{m} \Delta\boldsymbol{\sigma}_k^r = \sum_{k=1}^{m} (\Delta\boldsymbol{\sigma}_k^{exc} - \mathrm{d}\,\lambda_k \mathbf{D}\mathbf{a}_k) \,, \tag{35}$$

and the final reduced stress state $\boldsymbol{\sigma} = \boldsymbol{\sigma}^r$ is obtained as

$$\boldsymbol{\sigma}^r = \boldsymbol{\sigma}^C + \Delta\boldsymbol{\sigma}^r \,, \tag{36}$$

and must be located on the yield surface, that is $f(\boldsymbol{\sigma}^r) = Y$.

A detailed description of the numerical process applied in the computation of the stress state in an elasto-plastic regime is presented by Marques (1984).

7
Sensitivity analysis

To obtain the optimal design of composite structures under elasto-plastic loading conditions, it is necessary to perform the sensitivity analysis of the objective and the constraint functions. In this work the sensitivity analysis is performed using the Adjoint Variable Method. In the adjoint method, an augmented Lagrangian is defined in terms of adjoint variable fields. The adjoint variable fields are then defined so as to eliminate the implicit derivatives.

Following the method proposed by Arora and Cardoso (1992), considering a given constraint functional $G[\mathbf{d}(\mathbf{x}), \mathbf{x}]$ and rewriting the discretized nonlinear equation (19) of the path-dependent problem in following form:

$$\Psi \left[\boldsymbol{\sigma}^{(n)}(\mathbf{x}); \mathbf{d}^{(n)}(\mathbf{x}); \mathbf{x} \right] = \mathbf{r} \left[\boldsymbol{\sigma}^{(n)}(\mathbf{x}); \mathbf{d}^{(n)}(\mathbf{x}); \mathbf{x} \right] - \mathbf{F}^{(n)}(\mathbf{x}) \,, \tag{37}$$

the augmented constraint functional can be written as

$$L\left[\mathbf{d}^{(n)}(\mathbf{x})+\Delta\mathbf{d}(\mathbf{x});\boldsymbol{\Phi};\mathbf{x}\right]=G\left[\mathbf{d}^{(n)}(\mathbf{x})+\Delta\mathbf{d}(\mathbf{x});\mathbf{x}\right]-$$

$$\boldsymbol{\Phi}^T\Big\{\mathbf{r}\left[\boldsymbol{\sigma}^{(n+1)}(\mathbf{x});\mathbf{d}^{(n)}(\mathbf{x})+\Delta\mathbf{d}(\mathbf{x});\mathbf{x}\right]-$$

$$\mathbf{F}^{(n+1)}(\mathbf{x})\Big\}\,, \tag{38}$$

where $\mathbf{r}$ is the internal nodal force vector of the inelastic system and the argument $\mathbf{d}^{(n)}(\mathbf{x})+\Delta\mathbf{d}(\mathbf{x})$ have the same meaning as $\mathbf{d}^{(n+1)}(\mathbf{x})$. The vector of adjoint variables $\boldsymbol{\Phi}$ is assumed as the Lagrange multiplier and is selected in order to make stationary the functional L with respect to the displacement vector $\mathbf{d}$. This condition can be formulated as

$$\frac{\partial L}{\partial\mathbf{d}}=\frac{\partial G^{(n+1)}}{\partial\mathbf{d}}-\boldsymbol{\Phi}^T\frac{\partial\mathbf{r}^{n+1}}{\partial\mathbf{d}}=0\,. \tag{39}$$

Remembering from (28) that

$$\frac{\partial\Psi^{(n+1)}}{\partial\mathbf{d}}=\mathbf{K}_T^{(n+1)}\,, \tag{40}$$

where $K_T^{(n+1)}$ is the tangent stiffness matrix and considering the independence of $\mathbf{F}^{n+1}$ in order to the displacements $\mathbf{d}$, the adjoint set of equations is obtained

$$\mathbf{K}_T^{(n+1)}\boldsymbol{\Phi}=\frac{\partial G^{(n+1)}}{\partial\mathbf{d}}\,. \tag{41}$$

On other hand, taking into account that in an equilibrium situation the functional (37) is stationary, it is proven (Arora and Cardoso 1992) that

$$\frac{\mathrm{d}\,G}{\mathrm{d}\,\mathbf{x}}=\frac{\partial L}{\partial\mathbf{x}}\,. \tag{42}$$

Differentiating (38) in order to the design variables $\mathbf{x}$, we obtain

$$\frac{\partial L}{\partial\mathbf{x}}=\frac{\partial G^{(n+1)}}{\partial\mathbf{x}}+\frac{\partial G^{(n+1)}}{\partial\mathbf{d}}\frac{\partial\mathbf{d}^{(n+1)}}{\partial\mathbf{x}}+$$

$$\boldsymbol{\Phi}^T\left[\frac{\partial\mathbf{F}^{(n+1)}}{\partial\mathbf{x}}-\frac{\partial\mathbf{r}^{(n+1)}}{\partial\boldsymbol{\sigma}}\frac{\partial\boldsymbol{\sigma}^{(n+1)}}{\partial\mathbf{x}}-\right.$$

$$\left.\frac{\partial\mathbf{r}^{(n+1)}}{\partial\mathbf{d}}\frac{\partial\mathbf{d}^{(n+1)}}{\partial\mathbf{x}}-\frac{\partial\mathbf{r}^{(n+1)}}{\partial\mathbf{x}}\right]. \tag{43}$$

Considering the equality (39) it is obtained after simplification

$$\frac{\mathrm{d}\,G}{\mathrm{d}\,\mathbf{x}}=\frac{\partial L}{\partial\mathbf{x}}=\frac{\partial G^{(n+1)}}{\partial\mathbf{x}}+$$

$$\boldsymbol{\Phi}^T\left[\frac{\partial\mathbf{F}^{(n+1)}}{\partial\mathbf{x}}-\frac{\partial\mathbf{r}^{(n+1)}}{\partial\boldsymbol{\sigma}}\frac{\partial\boldsymbol{\sigma}^{(n+1)}}{\partial\mathbf{x}}-\frac{\partial\mathbf{r}^{(n+1)}}{\partial\mathbf{x}}\right]. \tag{44}$$

A most important consequence of sensitivity analysis for history-dependent problems is that the response sensitivity at given time depends on the structural response and sensitivities taken at previous time instants. The partial derivatives in (44) and the solution of the adjoint equation set in (41) can be obtained in an incremental manner at the same time as the equilibrim equations (37) but this process is expensive. Based on the assumption that the equilibrium system can be represented in a simplified manner, a more reliable process to apply the adjoint variable method is proposed. If we consider the discrete equilibrium equations of the structure through the relation

$$\mathbf{K}_S^{ep}\left(\mathbf{d}^{(n+1)},\boldsymbol{\sigma}^{(n+1)},\mathbf{x}\right)\mathbf{d}^{(n+1)}=\mathbf{r}^{(n+1)}\,, \tag{45}$$

where $\mathbf{K}_S^{ep}(\mathbf{d},\boldsymbol{\sigma},\mathbf{x})$ is the elasto-plastic secant stiffness matrix of the structural system under elasto-plastic loading conditions and considering (39) it can be written the adjoint system (41) in similar form as

$$\left[\frac{\partial\mathbf{K}_S^{ep}\left(\mathbf{d}^{(n+1)},\boldsymbol{\sigma}^{(n+1)},\mathbf{x}\right)}{\partial\mathbf{d}}\mathbf{d}^{(n+1)}+\right.$$

$$\left.\mathbf{K}_S^{ep}\left(\mathbf{d}^{(n+1)},\boldsymbol{\sigma}^{(n+1)},\mathbf{x}\right)\right]\boldsymbol{\Phi}=\frac{\partial G^{(n+1)}}{\partial\mathbf{d}}\,, \tag{46}$$

where

$$\left[\frac{\partial\mathbf{K}_S^{ep}\left(\mathbf{d}^{(n+1)},\boldsymbol{\sigma}^{(n+1)},\mathbf{x}\right)}{\partial\mathbf{d}}\mathbf{d}^{(n+1)}+\right.$$

$$\left.\mathbf{K}_S^{ep}\left(\mathbf{d}^{(n+1)},\boldsymbol{\sigma}^{(n+1)},\mathbf{x}\right)\right]=\mathbf{K}_T^{ep^{(n+1)}}\,, \tag{47}$$

that is the tangent stiffness matrix, similar to that obtained at the converged equilibrium solution, available after Newton-Raphson iterations.

On other hand, differentiating (45) in order of the design variables $\mathbf{x}$ and considering the independence between $\mathbf{x}$ and $\mathbf{d}$ as a consequence of the adjoint variable method, the following expression is obtained:

$$\frac{\partial\mathbf{K}_S^{ep}\left(\mathbf{d}^{(n+1)},\boldsymbol{\sigma}^{(n+1)},\mathbf{x}\right)}{\partial\mathbf{x}}\mathbf{d}^{(n+1)}=$$

$$\frac{\partial\mathbf{r}^{(n+1)}}{\partial\mathbf{x}}+\frac{\partial\mathbf{r}^{(n+1)}}{\partial\boldsymbol{\sigma}}\frac{\partial\boldsymbol{\sigma}^{(n+1)}}{\partial\mathbf{x}}\,. \tag{48}$$

The relation (44) can be rewritten in the following manner:

$$\frac{\mathrm{d}\,G}{\mathrm{d}\,\mathbf{x}}=\frac{\partial G^{(n+1)}}{\partial\mathbf{x}}+$$

$$\boldsymbol{\Phi}^T\left[\frac{\partial\mathbf{F}^{(n+1)}}{\partial\mathbf{x}}-\frac{\partial\mathbf{K}_S^{ep}\left(\mathbf{d}^{(n+1)},\boldsymbol{\sigma}^{(n+1)},\mathbf{x}\right)}{\partial\mathbf{x}}\mathbf{d}^{(n+1)}\right], \tag{49}$$

where the adjoint vector $\boldsymbol{\Phi}$ is obtained from the adjoint set of equations (41).

Considering that the elasto-plastic secant stiffness matrix of each element can be calculated as

$$\mathbf{K}_{S,e}^{ep}\left(\mathbf{d}^{(n+1)},\boldsymbol{\sigma}^{(n+1)},\mathbf{x}\right)=$$

$$\int_V \mathbf{B}_e\left(\mathbf{d}^{(n+1)}\right)^T \mathbf{D}_e^{ep}\left(\boldsymbol{\sigma}^{(n+1)},\mathbf{x}\right)\mathbf{B}_e\left(\mathbf{d}^{(n+1)}\right)\mathrm{d}\,V\,, \tag{50}$$

where the second subscript e denotes the element, (50) can be written after integration through the thickness of the element as

$$\mathbf{K}_{S,e}^{ep}\left(\mathbf{d}^{(n+1)},\boldsymbol{\sigma}^{(n+1)},\mathbf{x}\right)=$$

$$\int_A \mathbf{B}_e\left(\mathbf{d}^{(n+1)}\right)^T \overline{\mathbf{D}}_e^{ep}\left(\boldsymbol{\sigma}^{(n+1)},\mathbf{x}\right)\mathbf{B}_e\left(\mathbf{d}^{(n+1)}\right)\mathrm{d}\,A\,, \tag{51}$$

assuming that the $\mathbf{B}$ matrix is referred to the middle surface, A, of the element; under linear geometric assumptions $\mathbf{B}$ is a constant matrix. On the other hand it is

$$\overline{\mathbf{D}}_e^{ep}\left(\boldsymbol{\sigma}^{(n+1)},\mathbf{x}\right)=$$

$$\sum_{i=1}^{m}\left[Q_i(\overline{\mathbf{t}},\mathbf{h},\mathbf{w},\mathbf{z})\mathbf{D}_{ei}^{ep}\left(\boldsymbol{\sigma}^{(n+1)},\mathbf{x}\right)\right]\,, \tag{52}$$

where the elasto-plastic matrix $\mathbf{D}_{ei}^{ep}\left(\boldsymbol{\sigma}^{(n+1)},\mathbf{x}\right)$ is obtained from the equality (18), m is the number of layers of the laminate of e-element and $Q_i(\overline{\mathbf{t}},\mathbf{h},\mathbf{w},\mathbf{z})$ represents the dependence of the stiffness relatively to ply thickness $\overline{\mathbf{t}}$, to the height $\mathbf{h}$ and the width $\mathbf{w}$ of the beams and to the excentricity $\mathbf{z}$ of the ply referred to the middle surface of the plate element. In general it can be written $Q_i(\overline{\mathbf{t}},\mathbf{h},\mathbf{w},\mathbf{z})=Q_i(\mathbf{x})$.

The elasto-plastic stiffness derivative in (49) can be obtained in the following form:

$$\frac{\partial\mathbf{K}_{S,e}^{ep}\left(\mathbf{d}^{(n+1)},\boldsymbol{\sigma}^{(n+1)},\mathbf{x}\right)}{\partial\mathbf{x}}=$$

$$\int_A \mathbf{B}_e\left(\mathbf{d}^{(n+1)}\right)^T\frac{\partial\overline{\mathbf{D}}_e^{ep}\left(\boldsymbol{\sigma}^{(n+1)},\mathbf{x}\right)}{\partial\mathbf{x}}\mathbf{B}_e\left(\mathbf{d}^{(n+1)}\right)\mathrm{d}\,A\,, \tag{53}$$

with

$$\frac{\partial\overline{\mathbf{D}}_e^{ep}\left(\boldsymbol{\sigma}^{(n+1)},\mathbf{x}\right)}{\partial\mathbf{x}}=\sum_{i=1}^{m}\left[\frac{\partial Q_i(\mathbf{x})}{\partial\mathbf{x}}\mathbf{D}_{ei}^{ep}\left(\boldsymbol{\sigma}^{(n+1)},\mathbf{x}\right)+ Q_i(\mathbf{x})\frac{\partial\mathbf{D}_{ei}^{ep}\left(\boldsymbol{\sigma}^{(n+1)},\mathbf{x}\right)}{\partial\mathbf{x}}\right], \tag{54}$$

where m is the number of layers of the laminate of e-element and

$$\frac{\partial\mathbf{D}_{ei}^{ep}}{\partial\mathbf{x}}=\frac{\partial\mathbf{D}_{ei}^{e\ell}}{\partial\mathbf{x}}-\frac{1}{[(\mathbf{u}_D)^T\mathbf{a}]_{ei}}\times$$

$$\left\{2\mathbf{u}_D\left(\frac{\partial\mathbf{u}_D}{\partial\mathbf{x}}\right)^T-\frac{\frac{\partial}{\partial\mathbf{x}}\left[(\mathbf{u}_D)^T\mathbf{a}\right]}{(\mathbf{u}_D)^T\mathbf{a}}\mathbf{u}_D(\mathbf{u}_D)^T\right\}_{ei}\,, \tag{55}$$

with $\mathbf{u}_D=\mathbf{D}\mathbf{a}$, $\mathbf{a}$ being the flow vector. The finite element formulation is considered in order to obtain the partial derivatives, by direct differentiation, in the previous equations.

It is remarkable that the present analysis involves a history-dependent problem, and so the adjoint system defined through (41) and the expression (49) are established after the entire history of structural response has been generated and the constraints have been checked for violations.

Other crucial aspects of elasto-plastic sensitivity analysis, such as the possibly discontinuous nature of design gradients at transition points is discussed by Kleiber *et al.* (1997). In the realistic cases of structures with a great number of of integration points that do not enter the elasto-plastic range of material behaviour simultaneously but "one by one", the jumps become relatively small, generating errors that should also remain small.

8 Optimization process

8.1 Problem formulation

The structural system is divided into macroelements (substructures) as that used in the optimization method proposed by Conceição António *et al.* (1996) where there is one laminate for each macroelement. The optimal design problem of a statically loaded composite plate or shallow shell structures with reinforcement beams can be formulated as

$$\text{minimize } W(\overline{\mathbf{t}},\mathbf{h},\mathbf{w})\,, \tag{56}$$

subject to

$$g_j=\frac{d_k}{d_0}-1\le 0\,,\quad j=1,\ldots,N_d\,,$$

$$g_j=\frac{f(\boldsymbol{\sigma})_k}{Y}-1\le 0\,,\quad j=N_d+1,\ldots,N_d+N_s\,,$$

$$x_j^{\ell}\le x_j\le x_j^{u}\,,\quad j=N_s+1,\ldots,\overline{N}\,, \tag{57}$$

and the state equation

$$\Psi(\Theta, \overline{\mathbf{t}}, \mathbf{h}, \mathbf{w}, \mathbf{d}) = \int_V \mathbf{B}^T \boldsymbol{\sigma} \, \mathrm{d}\, V + \int_L \mathbf{B}_t^T M_{y'} \mathrm{d}\, L - \mathbf{F} =$$

$$\mathbf{r}(\Theta, \overline{\mathbf{t}}, \mathbf{h}, \mathbf{w}, \mathbf{d}) - \mathbf{F} = \mathbf{0}\,, \tag{58}$$

where N_d is the number of displacement constraints, N_s is the number of stress constraints in elastic loading conditions and $\overline{N}$ the total number of constraints. The objective function $W(\overline{\mathbf{t}}, \mathbf{h}, \mathbf{w})$ is the weight of the structure that represents a cost function, the design variables Θ and $\overline{\mathbf{t}}$ are, respectively, the ply angle vector and the ply thickness vector of the composite plate or shallow shell and the design variable vectors $\mathbf{h}$ and $\mathbf{w}$ are, respectively, the height and the width of the reinforcement beams. The parameters $\mathbf{d}_0$ and Y in (57) represent the allowable displacement and the yield stress. The last inequalities in (57) represent the size constraints and the symbols x_j^u and x_j^ℓ denote the upper and lower bounds, respectively.

It should be noted that the state equation simply represents the relationship between the design and state variables. This relationship is necessary since the constraints (57) cannot be expressed as explicit functions of the design variables only.

8.2 Decomposition of the problem

The optimization problem formulated at (56) to (58) is decomposed into two subproblems corresponding to the following levels.

8.2.1 First level

Solve in sequential form, for each load level $p^{(n)}$, the following subproblem:

maximize $E(\Theta)\,, \quad$ over $\Theta\,,$

subject to

$$\Psi^{(n)}(\Theta, \overline{\mathbf{t}}, \mathbf{h}, \mathbf{w}, \mathbf{d}) = \mathbf{r}^{(n)}(\Theta, \overline{\mathbf{t}}, \mathbf{h}, \mathbf{w}, \mathbf{d}) -$$

$$p^{(n)}\mathbf{F} = \mathbf{0}\,, \tag{59}$$

where $E(\Theta)$ is a structural efficiency estimator defined by

$$E(\Theta) = -\overline{g}(\Theta, \overline{\mathbf{t}}_0, \mathbf{h}_0, \mathbf{w}_0)\,, \tag{60}$$

with $\overline{g}$ depending on the elastic or plastic behaviour of the structure:

(i) in elastic loading conditions,

$$\overline{g} = \max(g_j\,,\ j = 1, \ldots, N_d + N_s)\,; \tag{61}$$

(ii) in plastic loading conditions the efficiency estimator is related with the plastic extension of the structure. In this approach the following relation is used:

$$\overline{g} = f_k(\boldsymbol{\sigma})\,, \tag{62}$$

where the k index is associated with the flow vector $\mathbf{a}$ as

$$\left\| \frac{\partial f_k(\boldsymbol{\sigma})}{\partial \boldsymbol{\sigma}} \right\|^2 = \max \left(\left\| \frac{\partial f_i(\boldsymbol{\sigma})}{\partial \boldsymbol{\sigma}} \right\|^2 \,,\ i = 1, \ldots, N_s \right)\,, \tag{63}$$

and N_s is the total number of points where the stress vector is evaluated.

This optimization subproblem is solved for the N_p load increments, being defined by the convergence conditions of the optimization process.

8.2.2 Second level

$$\text{Minimize } W(\overline{\mathbf{t}}, \mathbf{h}, \mathbf{w})\,, \text{over } \overline{\mathbf{t}}, \mathbf{h}, \text{ and } \mathbf{w}\,, \tag{64}$$

subject to

$$g_j(\Theta_0, \overline{\mathbf{t}}, \mathbf{h}, \mathbf{w}) = \frac{d_k}{d_0} - 1 \le 0\,, \quad j = 1, \ldots, N_d\,,$$

$$g_j(\Theta_0, \overline{\mathbf{t}}, \mathbf{h}, \mathbf{w}) = \frac{f(\boldsymbol{\sigma})_i}{Y} - 1 \le 0\,,$$

$$j = N_d + 1, \ldots, N_d + N_s\,,$$

$$x_j^l \le x_j \le x_j^u\,, \quad j = N_d + N_s + 1, \ldots, \overline{N}\,, \tag{65}$$

and the state equation

$$\Psi(\Theta_0, \overline{\mathbf{t}}, \mathbf{h}, \mathbf{w}) = \mathbf{0}\,. \tag{66}$$

8.3 Optimization algorithm

The optimization algorithm for the solution of the two subproblems, resulting from the decomposition, can be carried out according to the following steps.

8.3.1
First level

(1) Choose an initial solution, feasible or not.
(2) Considering the ply thicknesses of the plates or shallow shells, the height and the width of the reinforcement beams as constants, the objective function $E(\Theta)$ is maximized modifying the ply angles for the load level $p^{(n)}$, beginning with the optimal solution found for the previous load level $p^{(n-1)}$.
(3) If the local convergence criteria at this optimization level, based on the relative change of the design variable vector, is not satisfied return to step (2), else the process is halted after N_p load increments and go to the second level.

8.3.2
Second level

(4) Consider the initial solution as the final solution of the first optimization level.
(5) If the solution is feasible, the weight is minimized using the ply thicknesses of the plates or shallow shells, the height and width of the reinforcement beams while the constraints are not violated.
(6) If the solution is unfeasible, the search for an optimal solution is sought increasing the ply thicknesses of the plates or shallow shells, the height and width of the reinforcement beams until the constraints are checked.
(7) If the local convergence criteria at this level is not satisfied return to step (5) or (6).
(8) Check global convergence and return to step (2) if it is not satisfied. The global convergence criteria is based on relative change of weight function at the second level of the optimization process.

At the first optimization level the conjugate gradient method (Polack 1971) is used to obtain the solution of the efficiency maximization.

An optimality criteria presented by Soeiro *et al.* (1994) and Conceição António *et al.* (1996), is used at second level to perform the weight minimization. The method was developed based on the optimality condition that the most critical constraint g_j in (65) becomes active when the optimum is reached,

$$\overline{g}(\overline{\mathbf{t}}, \mathbf{h}, \mathbf{w}) - \overline{g}^{*} = 0\,, \tag{67}$$

with $\overline{g} = \max(\dots)$ and $\overline{g} = \max(g_j,\ j = 1, \dots, N_d + N_s)$ and $\overline{g}^{*}$ is the prescribed value.

The proposed approach is based on an heuristic decomposition of the space design together with a mixed incremental structural analysis/optimization procedure. The convergence conditions of the proposed double-level algorithm was shown by Conceição António *et al.* (1996).

9
Numerical examples

9.1
Example 1. Spherical shell

A spherical shallow shell was chosen as an example and Fig. 2 shows the geometric definition of the problem. The shell is hinged at its perimeter and subjected to a central point load $F_{\max}/4 = 55$ kN; only a quarter of the structure was considered for the numerical analysis. The vertical allowable displacement is $d_{\max} = 0.08$ m and it was not imposed any constraint related with the plastic zone on the structure. Lower and upper bounds of 0.001 m and 0.1 m, respectively, are imposed to the design variables $\overline{\mathbf{t}}$, $\mathbf{h}$ and $\mathbf{w}$.

The structure was divided into eight macroelements, four macroelements (1 to 4) grouping the shell elements and the others (5 to 8) grouping the beam elements, as shown in the Fig. 2. A symmetric laminate with six layers is considered for each shell/beam macroelement.

The mechanical properties of the material are presented in Table 1 where X and Y are the longitudinal and transversal strength, respectively, and S is the shear strength. The specific weight of the ply material is 1800 Kg/m^3. In this example it is not considered the work-hardening of the composite material.

Table 1 Mechanical properties of the layers of the laminates

E_1	E_2	G_{12}	ν
38.6 GPa	8.27 GPa	4.14 GPa	0.26
X	Y	S	
1062 MPa	31 MPa	72 MPa	

The sensitivity analysis plays an important role in the optimization process when it is performed using gradient based methods. Furthermore, in structural optimization regarding plasticity effects is very important the development of efficient sensitivity analysis with reliable computational costs.

For the validation of the sensitivity analysis model, based in the Adjoint Variable Method (AVM) proposed in Section 7, numerical tests were performed comparing the results of the present formulation with the ones obtained using the backward Finite Difference Method (FDM). A remarkable agreement is observed between the results as is shown in Figs. 3 and 4. Particular reference must be made to the evolution of the results with the increment of displacement and the extension of plastic zone on the structure.

The two optimization levels were performed in one stage of the design process because no further significant changes are observed in both optimization levels.

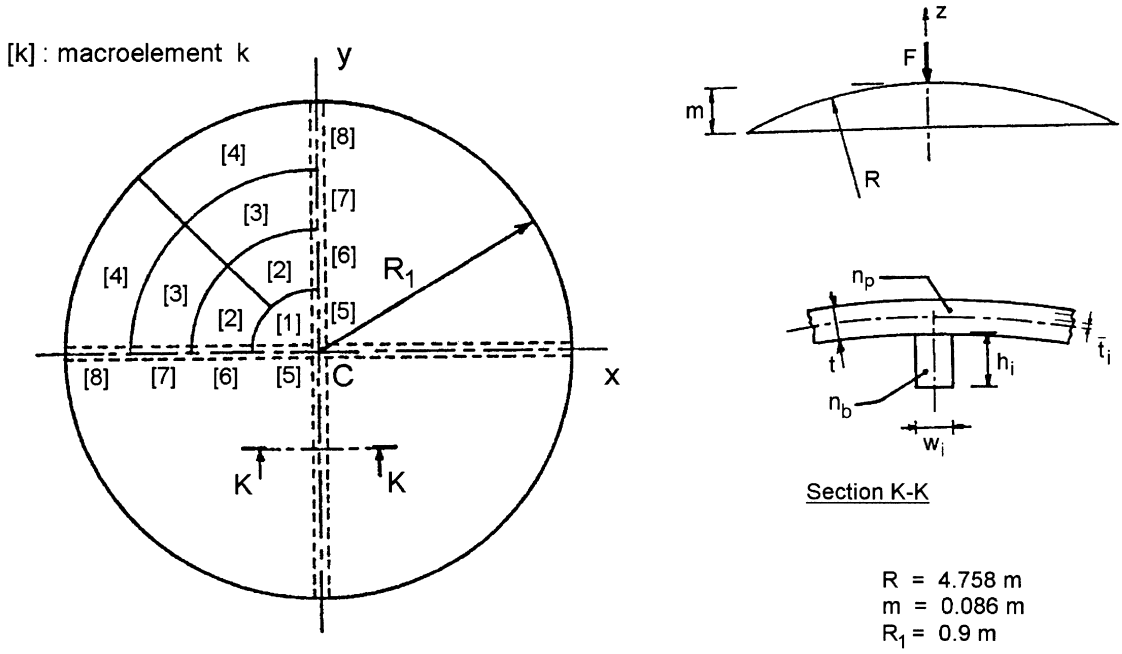

Fig. 2 Geometry and substructuring of spherical shallow shell

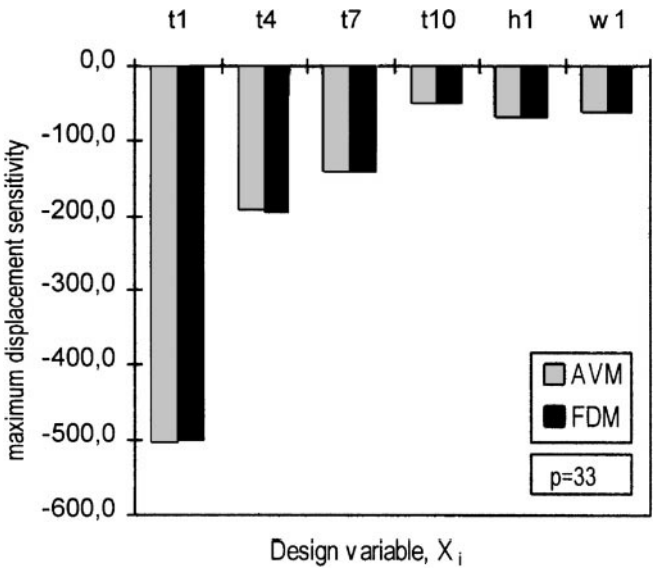

Fig. 3 Comparison of sensitivities for initial design at load level $f = 35$ KN and 33 plastic points

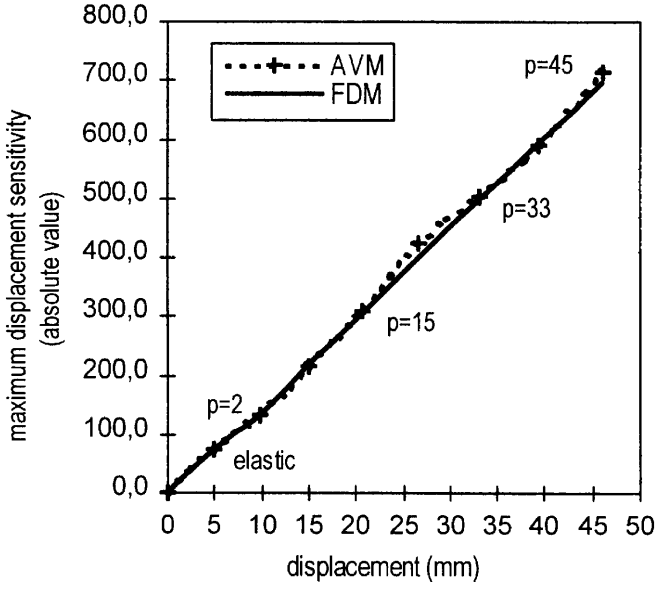

Fig. 4 Evolution of the sensitivities with the displacement and (p) plastic points for initial design

Figure 5 shows the recovered plastic zones at the first level of optimization process. The plastic points are associated with the Gaussian points localized in the midsection of each layer of the laminate. The load is applied in an incremental manner and the optimization process is restarted at each load level beginning with the optimal solution obtained at previous load level. It is remarkable that the optimization process is load path-dependent but reliable in the recovered plastic zones.

Figure 6 plots the curve force versus displacement reported to the loading point (at point C) for the first optimization level. Although the objective was not the displacement minimization, a displacement reduction for the same load level is observed.

Figures 7 and 8 are concern the second optimization level and represent the iterative histories of the weight and the most critical displacement (at point C). The convergence of the weight minimization process can be observed, with a reduction of 27% on the initial value of the

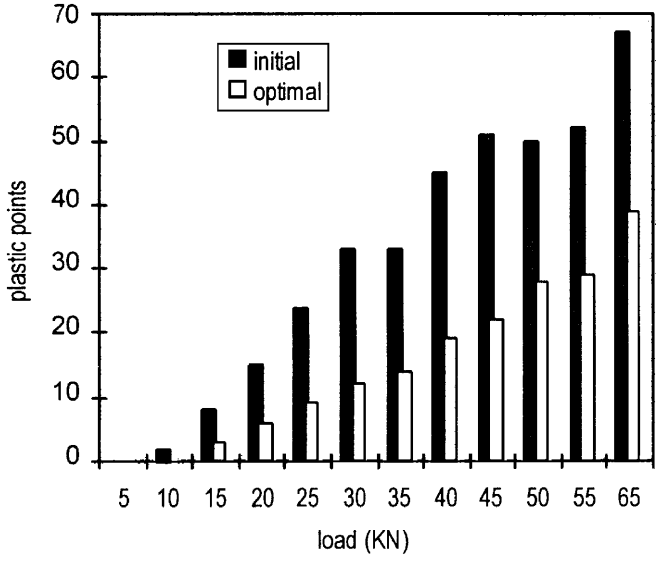

Fig. 5 Recovered plastic zones at the first level of the design process

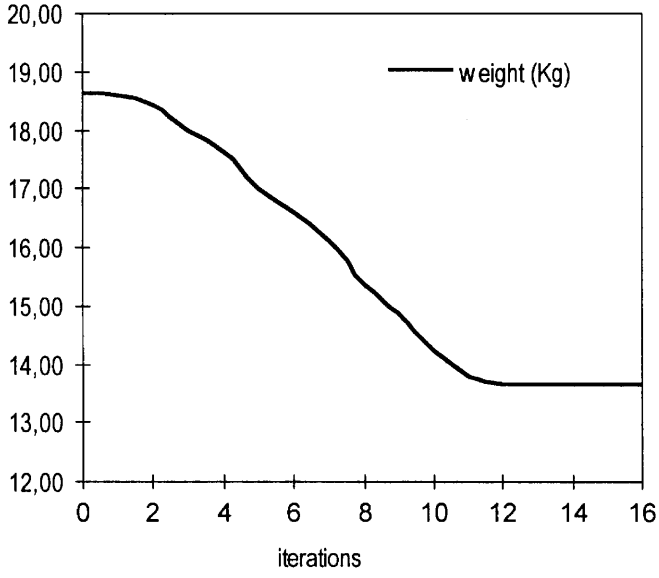

Fig. 7 Iterative history of the objective function at the second optimization level

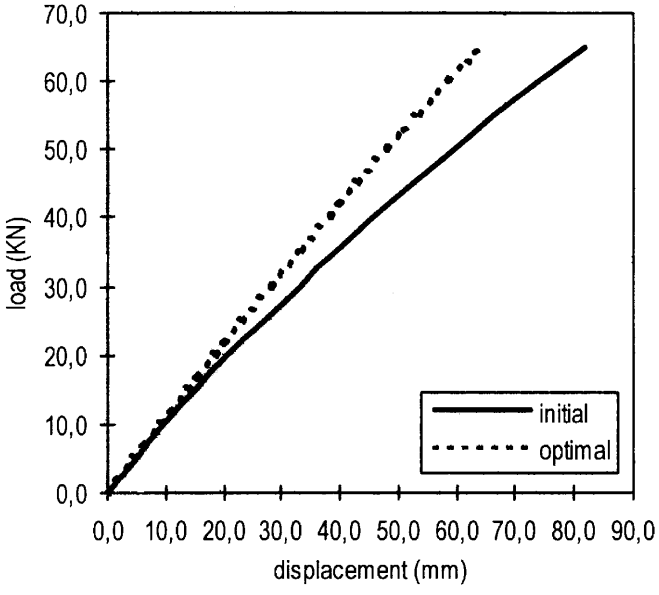

Fig. 6 Maximum displacement versus load at the first level of the design process

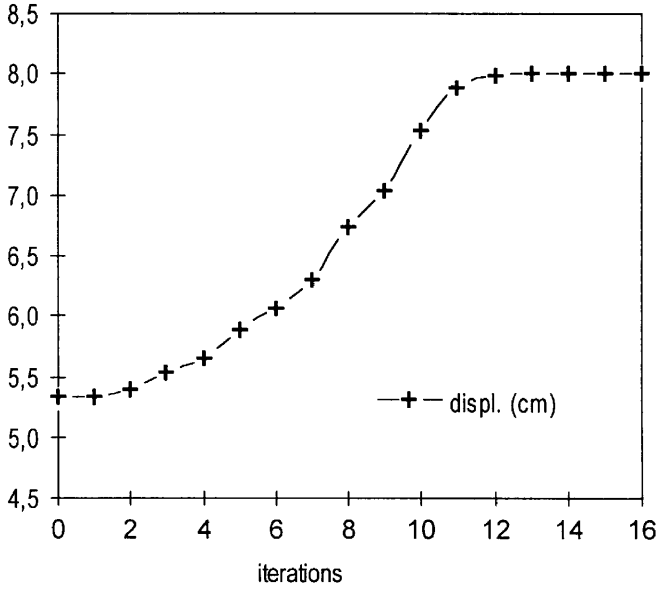

Fig. 8 Maximum displacement variation along the second optimization level

objective function, while the most critical constraint of displacement is satisfied. Table 2 presents the corresponding results for both optimization levels.

9.2 Example 2. Cylindrical shell

The second example considered in the analysis of the proposed approach is a cylindrical shallow shell, geometrically defined in Fig. 9. The shell is hinged at its straight borders and free on the curved ones. As in the previous example, only a quarter of the structure was considered for the numerical analysis and a central point load $F_{\max}/4 = 27.5$ kN is applied. The vertical allowable displacement is limited to $d_{\max} = 0.028$ m and no constraint related with the plastic zone extension on the structure was imposed. Lower and upper bounds of 5×10^{-4} m and 0.05 m, respectively, are imposed to the design variables $\overline{\mathbf{t}}$, $\mathbf{h}$ and $\mathbf{w}$.

This structure was divided in ten macroelements, four macroelements (1 to 4) grouping the shell elements and the other six macroelements (5 to 10) grouping the beam elements, as is shown in the Fig. 9. Each macroelement is

Table 2 Initial and optimal values for spherical shell ($\overline{t}_i$, h_i, w_i [mm] and Θ_i [degrees])

Macro element	Design variables	Initial design	Optimal design	Macro element	Design variables	Initial design	Optimal design
1	$\overline{t}_1/\Theta_1$	2.63 / 0.0	2.43 / 84.8	3	$\overline{t}_7/\Theta_7$	2.63 / 0.0	2.04 / 22.9
1	$\overline{t}_2/\Theta_2$	2.63 / 30.0	2.44 / 22.5	3	$\overline{t}_8/\Theta_8$	2.63 / 30.0	2.05 / 34.6
1	$\overline{t}_3/\Theta_3$	2.63 / 45.0	2.47 /−42.4	3	$\overline{t}_9/\Theta_9$	2.63 / 45.0	2.07 / 42.7
2	$\overline{t}_4/\Theta_4$	2.63 / 0.0	2.14 /−25.6	4	$\overline{t}_{10}/\Theta_{10}$	2.63 / 0.0	1.60 / 2.1
2	$\overline{t}_5/\Theta_5$	2.63 / 30.0	2.24 / 44.5	4	$\overline{t}_{11}/\Theta_{11}$	2.63 / 30.0	1.68 / 27.0
2	$\overline{t}_6/\Theta_6$	2.63 / 45.0	2.21 / 67.0	4	$\overline{t}_{12}/\Theta_{12}$	2.63 / 45.0	1.76 / 45.6
5	h_1/w_1	24.0 / 7.5	22.9 / 6.5	7	h_3/w_3	24.0 / 7.5	20.4 / 5.1
6	h_2/w_2	24.0 / 7.5	21.3 / 5.7	8	h_4/w_4	24.0 / 7.5	13.0 / 1.9

Table 3 Initial and optimal values for cylindrical shell ($\overline{t}_i$, h_i, w_i [mm] and Θ_i [degrees])

Macro element	Design variables	Initial design	Optimal design	Macro element	Design variables	Initial design	Optimal design
1	$\overline{t}_1/\Theta_1$	2.63 / 0.0	2.58 /−45.2	3	$\overline{t}_7/\Theta_7$	2.63 / 0.0	1.73 /−28.2
1	$\overline{t}_2/\Theta_2$	2.63 / 30.0	2.57 / 73.5	3	$\overline{t}_8/\Theta_8$	2.63 / 30.0	1.43 / 64.4
1	$\overline{t}_3/\Theta_3$	2.63 / 45.0	2.56 / 25.5	3	$\overline{t}_9/\Theta_9$	2.63 / 45.0	1.44 / 65.9
2	$\overline{t}_4/\Theta_4$	2.63 / 0.0	1.87 /−28.3	4	$\overline{t}_{10}/\Theta_{10}$	2.63 / 0.0	0.77 /−34.6
2	$\overline{t}_5/\Theta_5$	2.63 / 30.0	1.89 / 22.0	4	$\overline{t}_{11}/\Theta_{11}$	2.63 / 30.0	0.83 / 61.8
2	$\overline{t}_6/\Theta_6$	2.63 / 45.0	1.62 / 45.2	4	$\overline{t}_{12}/\Theta_{12}$	2.63 / 45.0	0.94 / 65.4
5	h_1/w_1	24.0 / 7.5	20.4 / 5.2	8	h_4/w_4	24.0 / 7.5	34.7 / 34.4
6	h_2/w_2	24.0 / 7.5	22.3 / 5.9	9	h_5/w_5	24.0 / 7.5	27.5 / 19.7
7	h_3/w_3	24.0 / 7.5	18.7 / 2.5	10	h_6/w_6	24.0 / 7.5	8.2 / 0.6

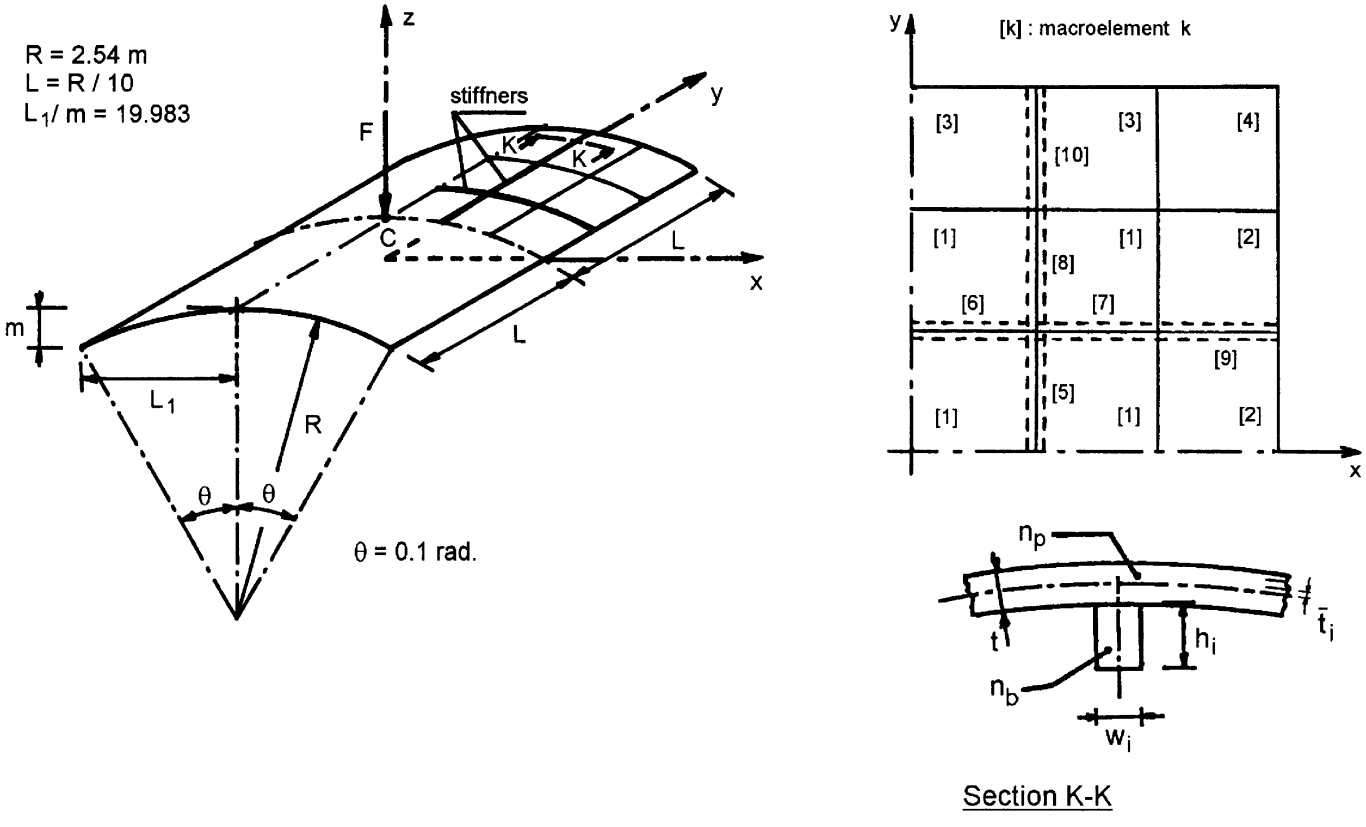

Fig. 9 Geometry and substructuring of cylindrical shallow shell

made of a symmetric shell/beam laminate with six layers, whose mechanical properties are defined in Table 1.

The two optimization levels were performed along two stages during the design process. The performance of the proposed approach can be evaluated through the Fig. 10 and Fig. 11. The first one shows the reduction observed in the extension of plastic zone at the first optimization level when the anisotropic characteristics of the laminates are manipulated.

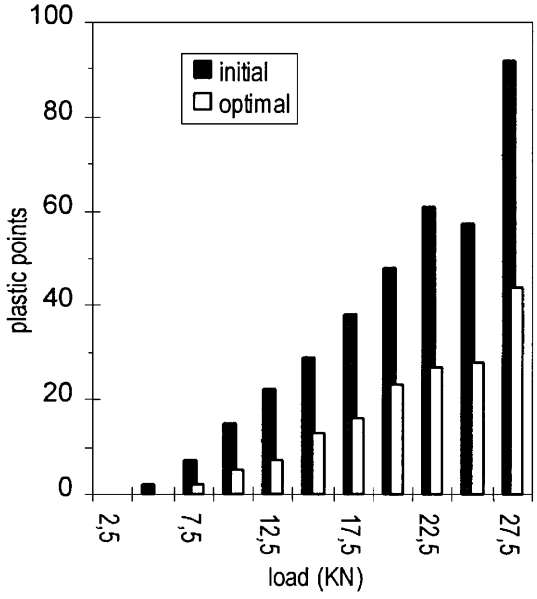

Fig. 10 Plastic points at the first level of the first stage of the design process

In Fig. 11 we can see the iterative history of the weight minimization, performed at second optimization level for each stage of the design process. It is noticed that each stage is started with the first level where the anisotropic characteristics are updated for better design.

At the final of second stage the structure have the optimal design present in Table 3. This configuration satisfies the prescribed displacement constraint while the plastic zone includes a total of 64 plastic points.

10 Conclusions

At elasto-plastic analysis of laminated composite structures made of thermoplastic resins gives a more realistic ultimate load carrying capacity than elastic analysis. Moreover it leads to more reasonable and economic structures.

The proposed approach for structural optimization of composite materials under elasto-plastic loading conditions seems to be an efficient way to obtain more reliable designs of composite structures. Indeed, the criterious manipulation of anisotropic characteristics and steacking sequence of the laminates and the geometric properties of reinforced beams, can lead to a reduction of the extension of plastic zones or the maximum displacement of the structure. These features have important consequences and benefits in what concerns the minimization costs, satisfaction of service conditions and structural integrity.

Acknowledgements The authors are grateful to the Fundação para a Ciência e a Tecnologia of Portugal by financial support provided.

References

Arora, J.S.; Cardoso, J.B. 1992: Variational principle for shape design sensitivity analysis. *AIAA J.* **30**, 538–547

Bathe, K.-J. 1996: *Finite element procedures*. Upper Saddle River, NJ, USA: Prentice-Hall

Conceição António, C.A.; Torres Marques, A.; Gonçalves, J.F. 1996: Reliability based design with a degradation model of laminated composite structures. *Struct. Optim.* **12**, 16–28

Crisfield, M.A. 1991: *Nonlinear finite element analysis of solids and structures 1*. Chichester, UK: John Wiley & Sons

Dvorak, G.J.; Bahei-El Din, Y.A. 1982: Plasticity analysis of fibrous composites. *ASME J. Appl. Mech.* **49**, 327–335

Fung, Y.C. 1965: *Foundations of solid mechanics*. Englwood Cliffs, NJ, USA: Prentice-Hall

Hill, R. 1950: *The mathematical theory of plasticity*. UK: Oxford University Press

Huang, H.-C. 1989: *Static and dynamic analyses of plates and shells*. Berlin, Heidelberg, New York: Springer

Kleiber, M.; Antúnez, H.; Hien, T.D.; Kowalczyk, P. 1997: *Parameter sensitivity in nonlinear mechanics: theory and finite element computations*. Chichester, England: John Wiley & Sons

Marguerre, K. 1938: Zur Theorie der gekrümmten Platte grosser Formänderung. In: *Proc. 5-th Int. Cong. Appl. Mech.*, pp. 93–101. London, UK: J. Wiley

Marques, J.M.M.C. 1984: Stress computation in elastoplasticity. *Int. J. Engng. Comp.* **1**, 42–51

Min, B.K. 1981: A plane stress formulation for elasto-plastic deformations of unidirectional composites. *J. Mech. Phys. Solids* **29**, 327–352

Oblak, M.M.; Kegl, M.; Butinar, B.J. 1993: An approach to optimal design of structures with nonlinear response. *Int. J. Num. Meth. Engrg.* **36**, 511–521

Ohsaki, M.; Arora, J.S. 1994: Design sensitivity analysis of elastoplastic structures. *Int. J. Num. Meth. Engrg.* **37**, 737–762

Owen, D.R.J.; Figueiras, J.A. 1983: Anisotropic elasto-plastic finite element analysis of thick and thin plates and shells. *Int. J. Num. Meth. Engng.* **19**, 541–566

Pica, A.; Wood, R.D. 1980: Postbuckling behaviour of plates and shells using a Mindlin shallow shell formulation. *Comp. & Struct.* **12**, 759–768

Pica, A.; Wood, R.D.; Hinton, E. 1980: Finite element analysis of geometrically nonlinear plate behaviour using a Mindlin formulation. *Comp. & Struct.* **11**, 203–215

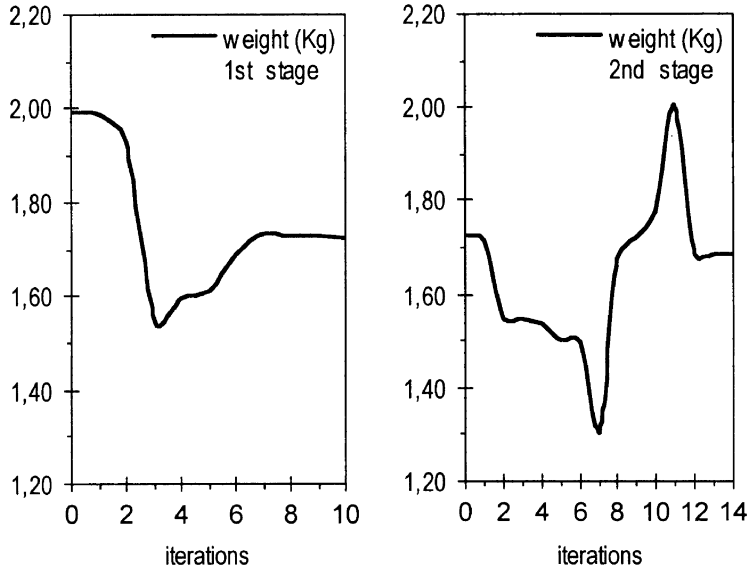

Fig. 11 Iterative history of the objective function at the second level of the design process

Polack, E. 1971: *Computational methods in optimization*. New York: Academic Press

Selyugin, S.V. 1995: Optimality criteria-based algorithms for plane-stress elasto-plastic structures. *Struct. Optim.* **9**, 207–213

Soeiro, A.V.; Conceição António, C.A.; Torres Marques, A. 1994: Multilevel optimization of laminated composite structures. *Struct. Optim.* **7**, 55–60

Tenney, D.R.; Disagor, W.B.; Dison, S.C. 1989: Materials and structures for hypersonic vehicules. *J. Aircraft* **26**, 953–970

Yoon, K.J.; Sun, C.T. 1991: Characterization of elasto-viscoplastic properties of an AS4/PEEK thermoplastic composite. *J. Composite Mat.* **25**, 1277–1296

Zienkiewicz, O.C.; Taylor, R.L. 1994: *The finite element method*. London: McGraw-Hill